Proceedings of the 21st ICSMGE, Vienna, Austria, 14 – 19 June 2026. Pistrol, Adam & Schweiger (eds.)
Published by: ÖGG, Austrian Society for Geomechanics, Salzburg, Austria, ISBN 978-3-9503898-4-5
https://doi.org/10.53243/ICSMGE2026-2089

Determination of Effective Strength Criteria for Random Geocomposites Using Finite Element Limit Analysis

Mariusz Myszor, Marek Kawa, Hubert Szabowicz
Faculty of Civil Engineering, Wroclaw University of Science and Technology, Poland, mariusz.myszor@pwr.edu.pl

ABSTRACT: The strength behavior of random composite materials, such as matrix–inclusion systems, is strongly influenced by their microstructural characteristics, particularly the size, geometry, and spatial distribution of inclusions within the matrix. While homogenization approaches for elastic and thermal properties are well established, the determination of effective strength parameters remains less explored. In this study, Finite Element Limit Analysis (FELA) is employed to numerically estimate the macroscopic load-bearing capacity of such materials. FELA provides a computationally efficient framework for assessing limit states by directly computing collapse loads, avoiding the complexity of full incremental elastoplastic simulations. The material is represented as a two-dimensional random matrix-inclusion type composite with a constant volume fraction, analyzed for three different inclusion sizes. Inclusions are randomly positioned within the matrix. All components are modeled using the Mohr–Coulomb failure criterion, commonly applied to granular and cohesive materials. For each configuration, a large number of random realizations is analysed under a wide range of loading programmes, which allows the complete averaged macroscopic failure surface and its statistical scatter (standard deviation) to be quantified in all loading directions. The results are expressed in terms of lower- and upper-bound failure surface estimates. The study provides a computational framework that can aid in developing strength homogenization approaches linking microstructural characteristics to macroscopic strength parameters.

KEYWORDS: Failure surface, limit analysis, geocomposite, strength, random microstructure.

1 INTRODUCTION

Heterogeneous materials, such as geocomposites with a granular structure, exhibit significant spatial variation of their properties at the microscale. Modeling such materials in full microstructural detail is computationally demanding and often unnecessary, particularly when the objective is to analyze their behavior at the structural scale. For the efficient modeling of such materials, a homogenization technique is required. Homogenization is a general framework—encompassing both analytical and numerical approaches—aimed at deriving effective material properties (e.g., stiffness, thermal conductivity) by averaging the spatially varying characteristics of the microstructure. The effective (averaged) properties obtained through the homogenization process allow a heterogeneous material to be replaced with an equivalent homogeneous continuum that reproduces the same macroscopic (or mesoscopic) response (see Fig. 1). This approach retains the macroscopic effects of the microstructural mechanical or physical characteristics while avoiding the complexity of explicitly modeling microstructural details.

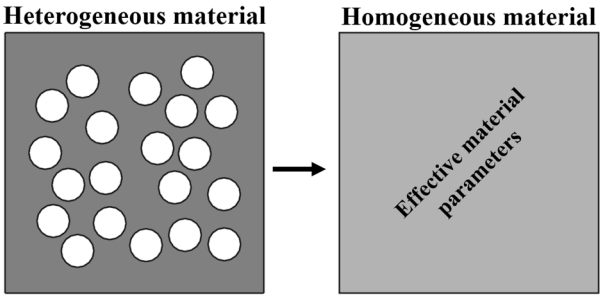

Figure 1. Concept of homogenization: replacing a heterogeneous composite microstructure with an equivalent homogeneous continuum described by effective material parameters.

Numerous homogenization techniques have been developed for estimating effective elastic moduli and thermal conductivity of heterogeneous materials, including analytical models (Ryu et al., 2019) and numerical approaches (Mortazavi et al., 2013). Such methods are routinely applied to composites to incorporate microstructural effects into macroscale analyses. However, the homogenization of strength parameters poses a fundamentally different challenge. Strength is governed by irreversible failure processes, which often initiate at the microscale due to stress concentration or local defects. While conventional homogenization approaches are effective for linear or reversible behavior, they are generally not suitable for accurately capturing damage or failure.

An essential step in strength homogenization is the determination of the failure surface, which characterizes the macroscopic strength behavior of the material. The failure surface provides a comprehensive description of the combinations of principal stresses at which the assumed limit state is reached (see Fig. 2). Such a representation can serve as a basis for formulating new macroscopic failure criteria that incorporate microstructural effects. For example, in granular materials governed by the Mohr–Coulomb (M–C) failure criterion, the failure surface can be parameterized in terms of the internal friction angle and cohesion. In the context of homogenization, these parameters become effective quantities, reflecting the averaged influence of microstructural heterogeneity.

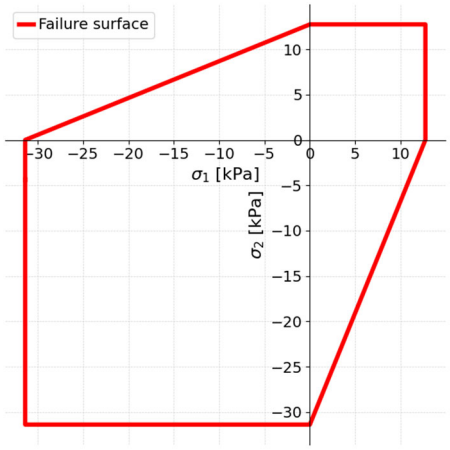

Figure 2. Two-dimensional Mohr–Coulomb failure surface in the principal stress space for a homogeneous material with an internal friction angle of 25° and cohesion of 10 kPa.

In this study, we address the problem of estimating the failure surface for random composites. To determine the averaged failure surface, simulations were performed for composite cells containing randomly distributed inclusions within the matrix with periodic boundary conditions. Each realization involved solving a boundary value problem in the context of strength analysis. Finite Element Method (FEM) simulations of such nonlinear problems are computationally demanding due to the iterative nature of the solution process. To overcome these limitations, we employed Finite Element Limit Analysis (FELA)—a numerical technique that enables relatively fast determination of the limit state without the need for incremental elastoplastic simulations. Preliminary results are presented for averaged failure surfaces obtained for composite cells containing circular inclusions with a constant volume fraction but varying diameters. In contrast to previous studies, where failure surface estimates are reported for a single composite cell realizations (e.g., Füssl et al., 2008), the present work evaluates the macroscopic failure surfaces estimates and its statistical scatter for all loading directions.

2 METHOD

2.1 *Finite Element Limit Analysis*

Finite Element Limit Analysis (FELA) is a computational approach based on the classical upper- and lower-bound theorems of plasticity, reformulated within a finite element framework. Unlike conventional Finite Element Methods (FEM), which simulate the full load–deformation path, FELA focuses exclusively on determining the ultimate load-carrying capacity. By assuming rigid–perfectly plastic material behavior, the method enables direct computation of collapse loads without tracking the complete constitutive response, which results in substantial computational efficiency.

In FELA, both the lower-bound (LB) and upper-bound (UB) estimates are obtained by solving convex optimization problems. The LB formulation (Sloan, 1988) seeks the maximum load multiplier for which a statically admissible stress field exists, satisfying equilibrium, boundary conditions, and a local yield criterion (e.g., Mohr–Coulomb). The UB formulation (Sloan, 1989) searches for the minimum load at which a kinematically admissible failure mechanism develops, defined by a displacement velocity field and the associated plastic flow rule.

This method has gained increasing popularity in geotechnical engineering (Lim et al., 2017; Vali et al., 2019; Chwała et al., 2024), especially through its implementation in commercial software (OPTUM G2, 2020), which provides a robust and efficient platform for practical applications. Compared to conventional FEM, FELA offers several advantages: it does not require a complete constitutive model; it avoids iterative load incrementation; and it yields mathematically rigorous bounds on the collapse load. In contrast, FEM results are sensitive to convergence criteria and provide no inherent guarantee of accuracy.

The strength parameters obtained from FELA simulations can be represented as a failure surface in the principal stress space (Fig. 3). This surface consists of discrete stress states, each corresponding to a specific loading program leading to collapse. For each loading program, FELA provides both LB and UB estimates of the limit load. The gap between these bounds reflects the discretization error, which is primarily influenced by the finite element mesh size, and can be reduced through the use of adaptive mesh refinement algorithms (Lyamin et al., 2005).

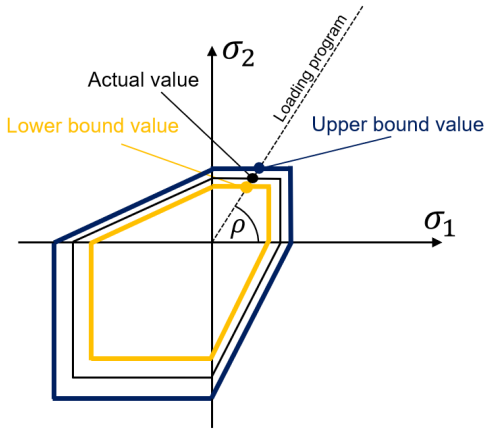

Figure 3. Schematic representation of the lower-bound (LB) and upper-bound (UB) solutions in Finite Element Limit Analysis (FELA) for a given loading program in the principal stress space.

2.2 *Model description and numerical procedure*

The analyses were limited to two dimensions under the assumption of plane stress conditions. Periodic boundary conditions were applied to the computational cell. Both the matrix material and the inclusions, as well as the interface between them, were modeled using the Mohr–Coulomb failure criterion. The matrix was assigned to higher strength parameters, whereas the circular inclusions represented material weakness zones characterized by lower values of internal friction angle and cohesion. The M-C parameters used for these two constituents are provided in Table 1.

Table 1. Material parameters used for the matrix and inclusion phases.

Parameter	Symbol	Value (matrix)	Value (inclusion)	Unit
Friction angle	φ	40	10	deg
Cohesion	c	20	2.5	kPa

The lower-bound (LB) formulation adopted in this study followed the approach of Lyamin and Sloan (2002), whereas the upper-bound (UB) formulation was based on the method of Makrodimopoulos and Martin (2008). In the LB analysis, the objective was to identify the maximum value of one of the principal stresses for a given loading program characterized by the angle ρ, which defined the relationship between the principal stresses. In contrast, the UB analysis sought the minimum value of the corresponding principal stress for the same loading program.

The computational model was discretized into triangular finite elements, with an identical mesh used for both LB and UB analyses. Linear shape functions were employed for the stress field in the LB formulation, whereas quadratic shape functions were applied for the displacement velocity field in the UB formulation.

The assumed orientation of the principal stresses and the finite element mesh for an example composite cell containing nine circular inclusions, are shown in Fig. 4. Both the matrix and inclusions are described by the Mohr–Coulomb failure criterion, with the matrix assigned higher strength parameters and the inclusions representing material weaknesses. The triangular finite element mesh corresponds to the discretization used in the analyses. For each realization, circular inclusions with a prescribed constant volume fraction were assumed. The inclusion centres were selected randomly within the cell, subject to the following geometric constraints: inclusions were not allowed to overlap, they could not intersect the model

boundaries, and the distance from any inclusion edge to the cell boundary had to be at least 5% of the cell width. Whenever a newly sampled inclusion centre violated any of these conditions, that centre was rejected and resampled, while all previously accepted inclusions were retained. Strength analyses of composite cells in which inclusions are allowed to intersect the cell boundaries are planned as part of future work.

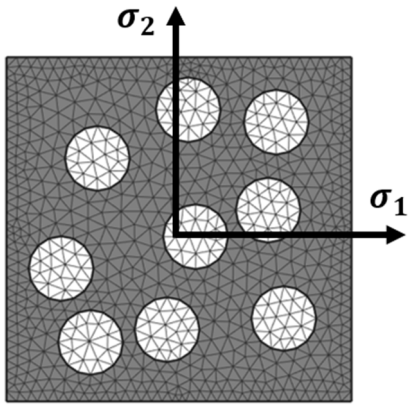

Figure 4. Example realization of a two-dimensional composite cell with nine circular inclusions.

All computations were conducted using custom MATLAB implementation, while the resulting optimization problems were solved with the commercial MOSEK software package. MOSEK is recognized as one of the most efficient solvers currently available for large-scale optimization tasks of this type (Podlich, 2017).

3 RESULTS

3.1 *Single composite cell*

For each realization, limit state analyses were carried out for a series of loading programs defined by the stress ratio $^{\sigma_2}/_{\sigma_1}$(equal to $\tan(\rho)$; see Fig. 3). The angle ρ was incremented in steps of 1° resulting in 360 for both lower and upper bound estimate.

Figure 5 presents a failure surface lower-bound estimate, which is conservative (safe), and an upper-bound estimate, both for the composite cell configuration shown in Fig. 4. As described earlier, the set of points in the principal stress space at which the assumed limit state is reached defines the failure surface. For the analyzed cell, these surface estimates have an overall shape similar to the Mohr–Coulomb criterion (see Fig. 2), with a noticeable difference in the form of rounded corners.

The difference between these results originates from the discretization of the numerical model. In the present case, the computational mesh consisted of approximately 2000 triangular elements, and for this mesh density, the relative variation between LB and UB strength estimates remained less than 15%.

Due to the random arrangement of inclusions, the composite material may exhibit anisotropic strength characteristics. This anisotropy is visible in the results, as the uniaxial compressive (or tensile) strength differs slightly between the vertical and horizontal loading directions.

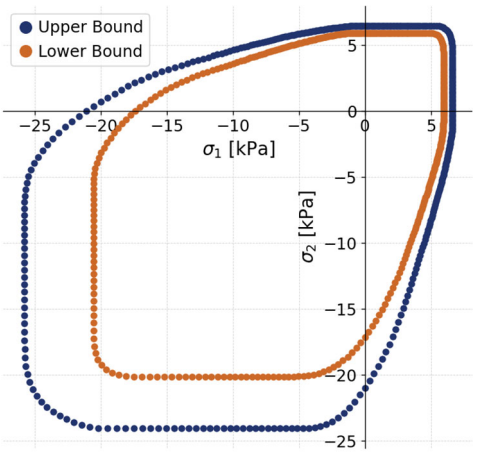

Figure 5. Lower-bound (orange) and upper-bound (blue) failure surface estimates obtained from Finite Element Limit Analysis (FELA) for a single realization of a two-dimensional composite cell with nine circular inclusions (configuration shown in Fig. 4).

3.2 *Average failure surface*

As mentioned earlier full analysis involved also changing dimensions of inclusions, while maintaining a constant inclusion volume fraction of 25%. The inclusion sizes for each configuration, expressed as the ratio of their diameter D to the cell edge length L, are summarized in Table 2.

Table 2. Geometrical parameters of composite cells with different inclusion sizes.

No. of inclusions	4	9	20
Size of the inclusion [D/L]	0.282	0.188	0.126

Figure 6 presents a graphical representation of the results obtained in the form of the average failure surfaces. Each data point represents the mean principal stress values calculated from 500 random realizations. Orange markers correspond to the lower-bound (LB) estimates and blue markers to the upper-bound (UB) estimates. The shaded region denotes the range of principal stress states within ±1 standard deviation from the mean.

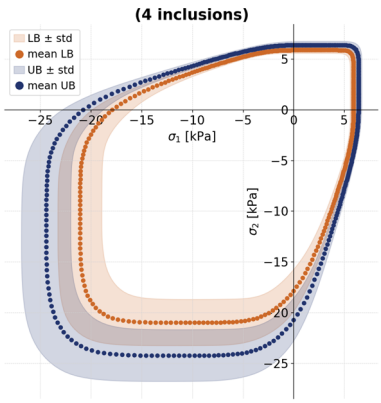

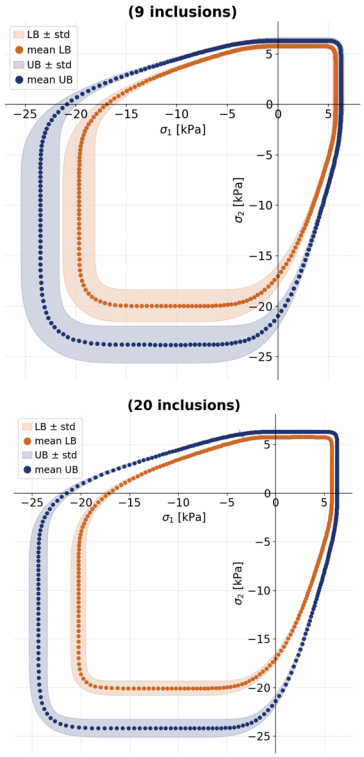

Figure 6. Average failure surfaces obtained from FELA simulations for three composite cell configurations with different inclusion sizes (see Table 2).

For the single realization shown in Fig. 5, the composite material exhibits a clear anisotropic strength response, with noticeable differences between the uniaxial strengths in the vertical and horizontal directions. However, when the results are averaged over 500 random realizations, the macroscopic response becomes effectively isotropic, as evidenced by the symmetry of the average failure surface estimates shown in Fig. 6.

A comparison of the results for the three composite cell configurations reveals that increasing the number of inclusions significantly reduces the scatter in the data, as indicated by the smaller standard deviation of the principal stress states. Although the magnitude of the standard deviation varies across the loading programs, the overall shape of the average failure surface estimates remains essentially unchanged, with only minor differences in the mean values.

4 CONCLUSIONS

In this study, a numerical framework based on Finite Element Limit Analysis (FELA) was applied to evaluate the macroscopic strength of random matrix-inclusion type composites. Three composite cell configurations with varying inclusion sizes but identical volume fraction were examined, each subjected to a large set of loading programs. For each configuration, 500 random realizations were generated, and both lower-bound and upper-bound estimates of the failure surface were determined.

The adopted computational methodology proved highly efficient for the strength assessments conducted in this work. In total, 1,080,000 limit analysis problems were solved, demonstrating that the proposed approach can deliver extensive statistical evaluations within practical computational times. Averaging the results over multiple random realizations was found to eliminate the apparent anisotropy observed in individual composite cells, leading to an effectively isotropic macroscopic failure surface.

Although the standard deviation of the principal stress states varied among the analyzed configurations, the general geometry of the average failure surface remained essentially unchanged, indicating that the overall average strength is robust to changes in inclusion size. Increasing the number of inclusions while maintaining the same volume fraction significantly reduced the scatter in the data.

From the standpoint of strength homogenization, the obtained average failure surfaces could provide a basis for determining effective values of internal friction angle and cohesion, which can be used to characterize the macroscopic strength of the heterogeneous composite. At the same time, further research should incorporate adaptive mesh refinement techniques to reduce the gap between lower- and upper-bound estimates, thereby improving the accuracy of the failure surface representation without a prohibitive increase in computational cost.

5 ACKNOWLEDGMENT

This work was supported by the Academia Professorum Iuniorum program at Wrocław University of Science and Technology (Grant No. 50AP/0010/25).

6 REFERENCES

Chwała, M., Komatsu, G., and Haruyama, J., 2024. Structural stability of lunar lava tubes with consideration of variable cross-section geometry. Icarus, 411, 115928.

Füssl, J., Lackner, R., Eberhardsteiner, J., and Mang, H.A., 2008. Failure modes and effective strength of two-phase materials determined by means of numerical limit analysis. *Acta Mechanica*, 195, 185–202.

Lim, K., Li, A.J., Schmid, A., and Lyamin, A.V., 2017. Slope-stability assessments using finite-element limit-analysis methods. International Journal of Geomechanics, 17(2), 06016017.

Lyamin, A.V., and Sloan, S.W., 2002. Lower bound limit analysis using non-linear programming. International Journal for Numerical Methods in Engineering, 55(5), 573-611.

Lyamin, A.V., Sloan, S.W., Krabbenhøft, K., and Hjiaj, M., 2005. Lower bound limit analysis with adaptive remeshing. *International Journal for Numerical Methods in Engineering*, 63(14), 1961-1974.

Makrodimopoulos, A., and Martin, C.M., 2008. Upper bound limit analysis using discontinuous quadratic displacement fields. Communications in Numerical Methods in Engineering, 24(11), 911-927.

Mortazavi, B., Baniassadi, M., Bardon, J., and Ahzi, S., 2013. Modeling of two-phase random composite materials by finite element, Mori–Tanaka and strong contrast methods. Composites Part B: Engineering, 45(1), 1117-1125.

Optum CE, 2020. OPTUM G2. Version 2020. Optum Computational Engineering. Computer software. Available at: www.optumce.com/

Podlich, N.C., 2017. The development of efficient algorithms for large-scale finite element limit analysis. PhD thesis, University of Newcastle.

Ryu, S., Lee, S., Jung, J., Lee, J., and Kim, Y., 2019. Micromechanics-based homogenization of the effective physical properties of composites with an anisotropic matrix and interfacial imperfections. Frontiers in Materials, 6, 21.

Sloan, S.W., 1988. Lower bound limit analysis using finite elements and linear programming. International Journal for Numerical and Analytical Methods in Geomechanics, 12(1), 61-77.

Sloan, S.W., 1989. Upper bound limit analysis using finite elements and linear programming. International Journal for Numerical and Analytical Methods in Geomechanics, 13(3), 263-282.

The MathWorks, Inc., 2024. MATLAB Version R2024b. Computer software. Available at: https://www.mathworks.com/

Vali, R., Beygi, M., Saberian, M., and Li, J., 2019. Bearing capacity of ring foundation due to various loading positions by finite element limit analysis. Computers and Geotechnics, 110, 94-113.